Journal of Alloys and Compounds 489 (2010) 110–114

Contents lists available at ScienceDirect

Journal of Alloys and Compounds

journal homepage: www.elsevier.com/locate/jallcom

Magnetic and structural properties of $BaFe_{12-x}Ga_xO_{19}$ nanoparticles

I. Bsoul[a,*], S.H. Mahmood[b,1]

[a] Physics Department, Al al-Bayt University, Mafraq 130040, Jordan
[b] Physics Department, Yarmouk University, Irbid 211-63, Jordan

ARTICLE INFO

Article history:
Received 24 June 2009
Received in revised form 3 September 2009
Accepted 4 September 2009
Available online 11 September 2009

Keywords:
Ball milling
Barium ferrite
Coercive field
Magnetization

ABSTRACT

The structural and magnetic properties of barium hexaferrite nanoparticles ($BaFe_{12-x}Ga_xO_{19}$) with $x = 0.0$–1.0, prepared by ball milling were investigated using XRD, TEM, and VSM. It was found that the particles and crystallites have similar mean size of ~41 nm for all investigated samples. The saturation magnetization decreased slightly and nonlinearly with increasing x, and this was attributed to different preferential site occupation of Ga at low and high concentration ranges. The coercivity decreased slightly with increasing x for low concentrations of Ga ($x \leq 0.2$), and then increased with increasing Ga concentration up to $x = 1.0$. This behavior of the coercivity was attributed to the change in the exchange coupling, which was confirmed by the variation of SFD, remanence ratio and Curie temperature with Ga concentration in the samples.

1. Introduction

Barium hexaferrite with its stoichiometric chemical formula $BaFe_{12}O_{19}$ is one of M-type hexaferrites (BaM). M-type hexaferrites have large saturation magnetization, high coercivity, high Curie temperature, large uniaxial magnetic anisotropy and excellent chemical stability. These materials have been intensively investigated due to their technological applications in permanent magnets, high-density magnetic recording media and microwave devices. Several techniques have been used to prepare hexaferrite particles including sol–gel method [1–3], citrate–nitrate gel combustion method [4], ammonium nitrate melt technique [5,6], mechano-combustion route [7], co-precipitation method [8], and microwave-induced hydrothermal reaction [9]. Several studies on hexaferrites in which Fe ions are substituted by different cations or combinations of cations have been carried out to develop materials with improved characteristics suitable for technological applications. Among the recently investigated substitutions are Mn–Co–Zr [10], Ni–Ti [11], Gd–Co [12], Co–Ti [13–15], Co–Zr [16], Zr–Zn [17], Mn and Ti [18].

The present work is concerned with the magnetic properties of BaM doped with gallium. The samples were prepared by ball milling, which had been recently used to prepare barium ferrite powders. This method is simple and useful for the production of powders consisting of fine particles smaller than the critical single domain size. The magnetic, XRD and TEM data were analyzed in an attempt to explain the magnetic behavior of $BaFe_{12-x}Ga_xO_{19}$.

2. Experimental procedures

$BaFe_{12-x}Ga_xO_{19}$ powders with $x = 0.0$, 0.2, 0.4, 0.6, 0.8 and 1.0 were prepared by ball milling. Metallic oxides (Fe_2O_3, and Ga_2O_3) and barium carbonate ($BaCO_3$) were used as starting materials. Mechanical alloying was carried out in a planetary ball mill (Fritsch Pulverisette 7) using a ball to powder ratio of 8:1. The milling was carried out for 24 h with an angular frequency of 250 rpm. After mechanical milling, the powders were pressed under a force of 50 kN into disks, 1 cm in diameter each. These disks were annealed in air at 1100 °C for 2 h.

XRD analysis was carried out using Philips X'Pert PRO X-ray diffractometer (PW3040/60) with CuKα radiation. XRD patterns for the samples examined were recorded in the range of 2θ between 15° and 75° with scanning step of 0.017°. A powder diffraction software package which includes the standards of the International Center for Diffraction Data (ICDD) was used to identify the observed structural phases. Transmission electron microscopy (TEM) using Zeiss EM10CR electron microscope operating at 80 kV was employed for estimating the particle sizes. TEM samples were prepared by suspending the powders in ethanol and shaking the suspension ultrasonically for several minutes. The suspension of the samples sintered at 1100 °C was immediately light-brown colored, indicating the fine particle nature of the investigated samples. A drop of the suspension on a formvar-coated copper TEM grid was allowed to dry in air before starting the measurements. The magnetic measurements were carried out using a vibrating sample magnetometer (VSM MicroMag 3900, Princeton Measurements Corporation). The saturation magnetization (M_s) was obtained from the extrapolation of the magnetization curve versus $1/H$ to $1/H = 0$. The switching field distribution (SFD) for each sample was determined by differentiation and normalization of the DC demagnetization curve (DCD). The remanence coercivity (H_{cr}) was determined from the normalized DCD curve.

3. Results and discussion

Fig. 1 shows the XRD patterns of samples of $BaFe_{12-x}Ga_xO_{19}$ along with the standard pattern for hexagonal barium ferrite

* Corresponding author. Tel.: +962 2 6297000x2127; fax: +962 2 6297031.
E-mail addresses: Ibrahimbsoul@yahoo.com (I. Bsoul), mahmoods@yu.edu.jo (S.H. Mahmood).
[1] Tel.: +962 2 721 1111x2071; fax: +962 2 721 1121.

0925-8388/$ – see front matter © 2009 Elsevier B.V. All rights reserved.
doi:10.1016/j.jallcom.2009.09.024

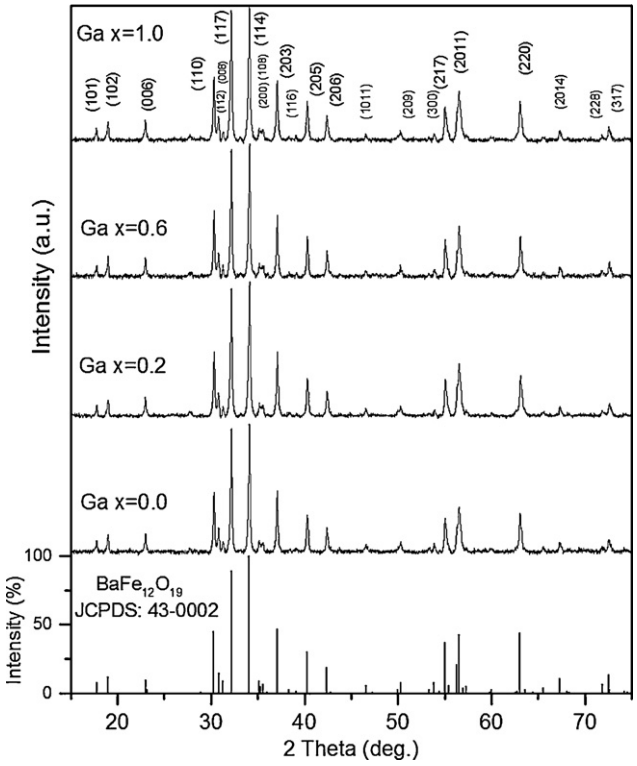

Fig. 1. Standard JCPDS pattern for M-type hexagonal barium ferrite (file no.: 043-0002) and XRD patterns of $BaFe_{12-x}Ga_xO_{19}$ with different doping concentration.

($BaFe_{12}O_{19}$) with space group $P6_3/mmc$ (JCPDS file no.: 043-0002) [19]. The figure shows that the XRD patterns for all samples exactly match the standard 043-0002 for hexagonal barium ferrite ($BaFe_{12}O_{19}$) with no secondary phases, which indicates that Ga^{3+} ions diffused into the hexagonal structure forming a single hexagonal $BaFe_{12-x}Ga_xO_{19}$ phase for all values of x. The lattice parameters a and c of this phase were calculated from the formula [20]:

$$\frac{1}{d^2_{h\,k\,l}} = \frac{4}{3}\left(\frac{h^2+hk+k^2}{a^2}\right) + \frac{l^2}{c^2} \quad (1)$$

where d is the interplanar distance and h, k, and l are Miller indices. The lattice parameters of Ga substituted barium hexaferrites (Table 1) show variations less than 0.1%. This is expected because the radius of Ga^{3+} ion (0.625 Å) is almost equal to that of Fe^{3+} (0.645 Å).

The average crystallite size was determined from the positions of the peaks (1 1 4), (2 1 7) and (2 2 0) using the well-known Scherrer formula [21]:

$$D = \frac{k\lambda}{\beta \cos\theta}, \quad (2)$$

where D is the crystallite size, k the Scherrer constant, λ the wavelength of radiation (1.54056 Å), β the peak width at half maximum measured in radians, and θ the peak position. The average crystallite size for the pure and doped samples (Table 1) ranges from 37 nm to 45 nm.

Table 1
Lattice parameters and average crystallite sizes of $BaFe_{12-x}Ga_xO_{19}$ measured by XRD.

x	a (Å)	c (Å)	c/a	Average crystallite size, D (nm)
0.0	5.890	23.194	3.938	45
0.2	5.887	23.203	3.942	44
0.4	5.886	23.208	3.943	39
0.6	5.888	23.199	3.940	44
0.8	5.891	23.206	3.939	40
1.0	5.890	23.207	3.940	37

Table 2
Coersivity, saturation magnetization, remanence ratio M_{rs} (M_r/M_s) and Curie temperature for $BaFe_{12-x}Ga_xO_{19}$.

x	H_c (kOe)	M_s (emu/g)	M_{rs}	T_c (°C)
0.0	4.02	70.9	0.523	505
0.2	3.95	69.3	0.519	500
0.4	4.00	68.3	0.518	490
0.6	4.26	68.0	0.519	470
0.8	4.49	65.3	0.517	455
1.0	4.55	60.3	0.514	415

TEM images of representative samples are shown in Fig. 2. The average particle size for the pure sample is 42 ± 13 nm, and for the sample with $x = 1.0$ is 41 ± 13 nm. These values are much smaller than the critical value of 460 nm reported by Rezlescu et al. [22] for single magnetic domain structure. Subsequently, we carried out magnetization measurements on the pure barium ferrite sample annealed at 1350 °C for 4 h and the results are shown in Fig. 3 together with those for the sample annealed at 1100 °C. The figure demonstrates that the magnetization of the sample annealed at 1100 °C increases slowly at low fields followed by a rapid increase at higher fields. This behavior is typical for randomly oriented single domain magnetic particles. In contrast, the initial magnetization for the pure sample annealed at 1350 °C shows a sharp increase at low fields then continues to increase slowly at higher fields. This behavior is typical for multi-domain particles. Further, attempts to suspend the powder of the sample annealed at 1350 °C in ethanol for TEM measurements failed, indicating that this powder consists of large particles. These observations indicate that ball milling method is suitable for preparing single domain magnetic nanoparticles with a narrow particle size distribution suitable for high-density recording applications.

Hysteresis loops for $BaFe_{12-x}Ga_xO_{19}$ samples are measured as a function of applied magnetic field and the results are shown in Table 2. The magnetization for the non-substituted sample is characteristic of hard magnetic material with coercive field of about 4 kOe. This value of the coercivity agrees well with previous results on samples prepared by sol–gel method [23] and mechanical alloying method [24].

The influence of Ga content on the saturation magnetization and coercivity of $BaFe_{12-x}Ga_xO_{19}$ is also shown in Fig. 4. The saturation magnetization decreases slowly for $x = 0.0 - 0.6$ (decrease in M_s is 2.5%). For $x \geq 0.6$, M_s drops faster, recording a reduction in M_s of 11% at $x = 1.0$. This decrease in M_s is still small compared with the reduction of 50% due to doping barium ferrites with Cr^{3+} [25]. The magnetic moment per formula for barium hexaferrite had been calculated from the sum of the magnetic moments of Fe ions in the different crystallographic sites as follows [26–28]:

$$\vec{m} = \overrightarrow{2a} + \overrightarrow{2b} + \overrightarrow{12k} + \leftarrow 4f_1 + \leftarrow 4f_2 \quad (3)$$

The spin-down sites ($4f_1$ and $4f_2$) are occupied by two Fe ions each, whereas the spin-up sites $2a$ and $2b$ are occupied by one Fe ion each, and $12k$ is occupied by six Fe ions. Based on this simple model, the magnetic moment of the pure phase is $4 \times 5\mu_B = 20\mu_B$ per formula. Accordingly, replacement of spin-up Fe ions by non-magnetic Ga ions would result in a drop of the magnetic moment down to $17\mu_B$ per formula (15% drop of the magnetization) for $x = 0.6$, and to $15\mu_B$ per formula (25% drop of the magnetization) for $x = 1.0$. These values are significantly higher than the observed drop in magnetization, indicating that replacement of Fe ions by Ga occurs at both spin-up and spin-down sites, with a preference for replacement at the spin-up sites. The observed values of the drop in magnetization at $x = 0.6$ and 1.0, and the behavior of the magnetization in this concentration range suggest that the fraction of Ga ions replacing

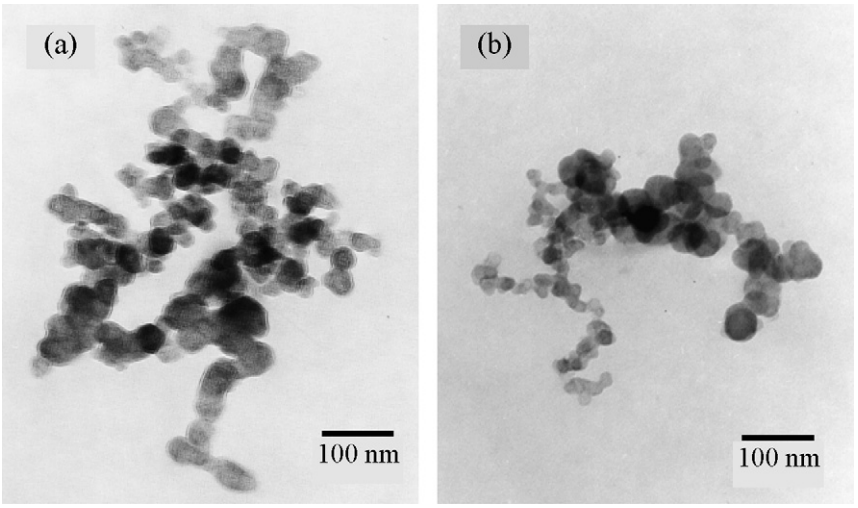

Fig. 2. TEM images of $BaFe_{12-x}Ga_xO_{19}$: (a) $x = 0.0$ and (b) $x = 1.0$.

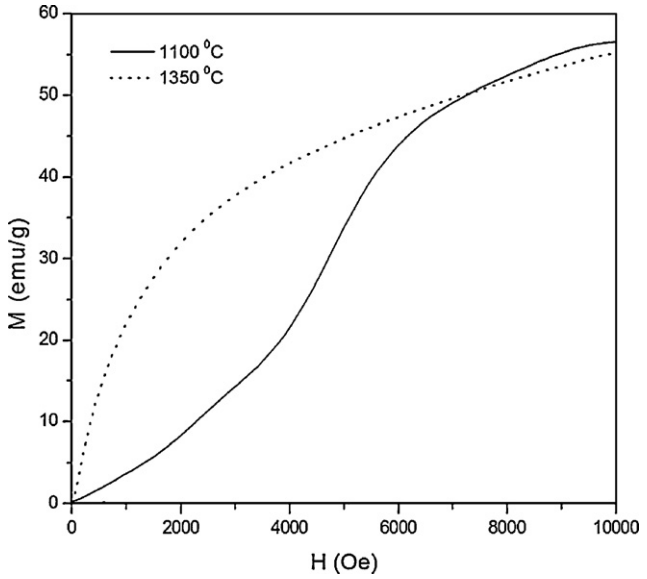

Fig. 3. Initial magnetization curves for pure barium ferrite samples ($x = 0.0$) annealed at 1100 °C for 1 h and 1350 °C for 4 h.

Fe ions at the spin-down sites increases with x reaching a value of 0.25 at $x = 0.6$, and remains constant at higher x values. Accordingly, only 0.35 Ga ions occupy spin-up sites at $x = 0.6$, and 0.75 Ga ions occupy spin-up sites at $x = 1.0$. Further, the change of behavior of the magnetization with Ga concentration at $x = 0.6$ could be due to the attenuation of the superexchange interaction between Fe^{3+} ions at tetrahedral and octahedral sites as a result of the excessive replacement of the magnetic ions by non-magnetic ones [29]. However, the marginal drop in magnetization in our system suggests that hexaferrite nanoparticles doped with small amounts of Ga (up to 0.6) have high M_s values necessary for various applications.

Fig. 4 also shows that with increasing Ga doping, the value of the coercivity decrease slightly between $x = 0.0$ and $x = 0.2$, and then increases monotonically for $x \geq 0.2$. This behavior and the apparent decrease in M_{rs} ($=M_r/M_s$) with Ga concentration can be associated with the attenuation of the exchange coupling, which leads to a decrease in remanence ratio and an increase in the coercive field, and results in a wider SFD [30]. Fig. 5 shows a representative reduced DCD curve (m_d) and the corresponding SFD for the sample with $x = 1.0$. From this figure we can find the remanence coercivity and the full width at half maximum (FWHM) of the SFD. Fig. 6 shows the FWHM of the SFD and H_{cr} as a function of Ga concentration for

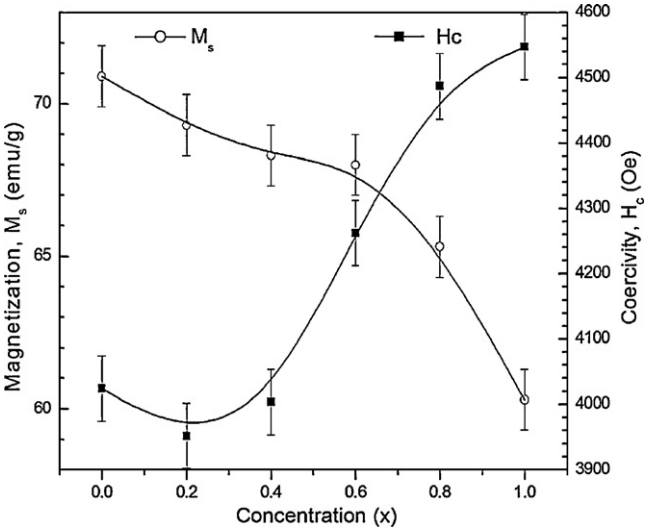

Fig. 4. Saturation magnetization and coercivity of $BaFe_{12-x}Ga_xO_{19}$ as a function of Ga concentration (x).

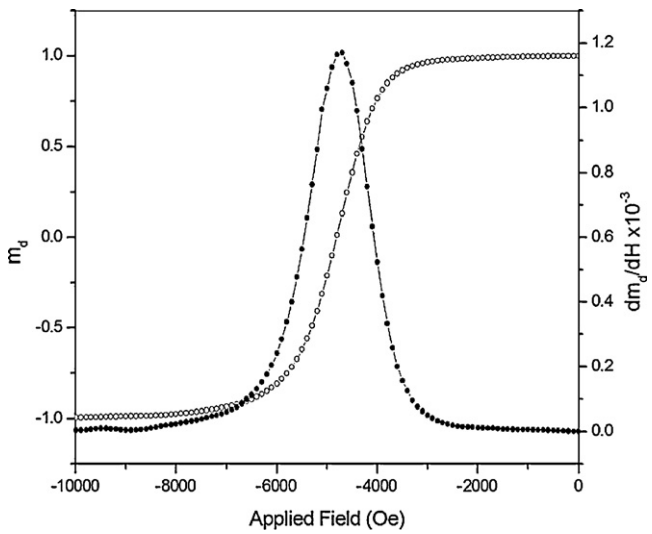

Fig. 5. Reduced DCD curve and switching field distribution for the sample with $x = 1.0$.

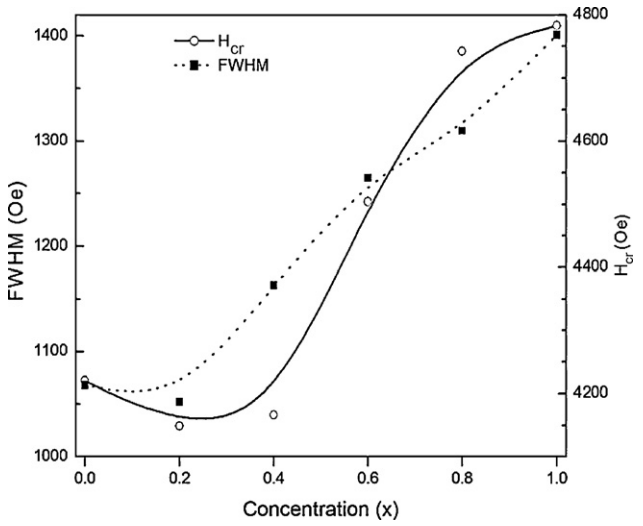

Fig. 6. FWHM and H_{cr} as a function of the Ga concentration for $BaFe_{12-x}Ga_xO_{19}$.

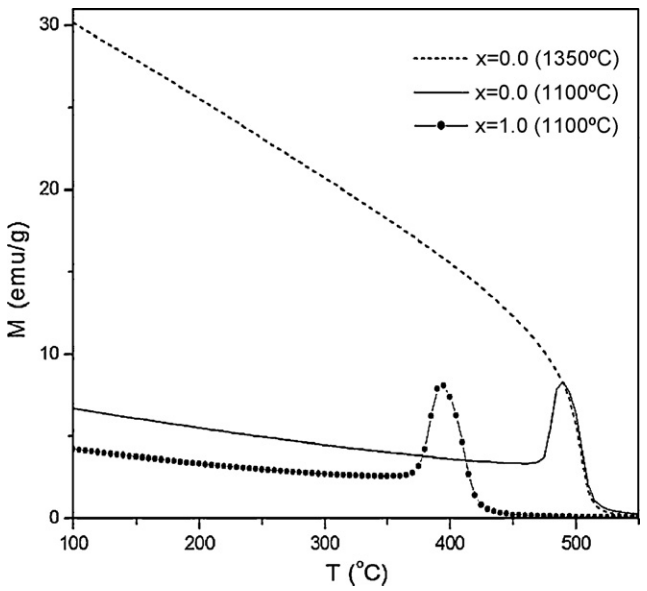

Fig. 8. Magnetization versus temperature (at constant applied field of 2 kOe) for the samples with $x = 0$ and $x = 1.0$ annealed at 1100 °C and for the sample with $x = 0$ annealed at 1350 °C.

all samples examined in this work. It is clear that the variations of both FWHM and H_{cr} with Ga doping display similar behavior, and are consistent with the attenuation of the magnetic exchange coupling with increasing Ga content. Further, a reduction in Curie temperature (T_c) is expected as a result of Ga doping. Fig. 7 shows representative magnetization curves as a function of temperature for the samples with $x = 0.0$, 0.6 and 1.0 at a constant applied field of 8 kOe. From these curves one might obtain T_c, which is defined as the temperature at the inflection point of the curve of the magnetization versus temperature. Curie temperature as a function of Ga concentration in $BaFe_{12-x}Ga_xO_{19}$ is shown in Table 2. Since the hexagonal structure and the morphology and average particle size in all samples examined in this work do not change appreciably, the decrease of T_c is consistent with the conclusion that the replacement of Fe ions by Ga ions results in the attenuation of the magnetic exchange coupling.

Fig. 8 shows the magnetization versus temperature for the samples with $x = 0$ and $x = 1.0$ annealed at 1100 °C, and for the sample with $x = 0$ annealed at 1350 °C in an applied field of 2 kOe. Both curves of the samples annealed at 1100 °C show Hopkinson effect

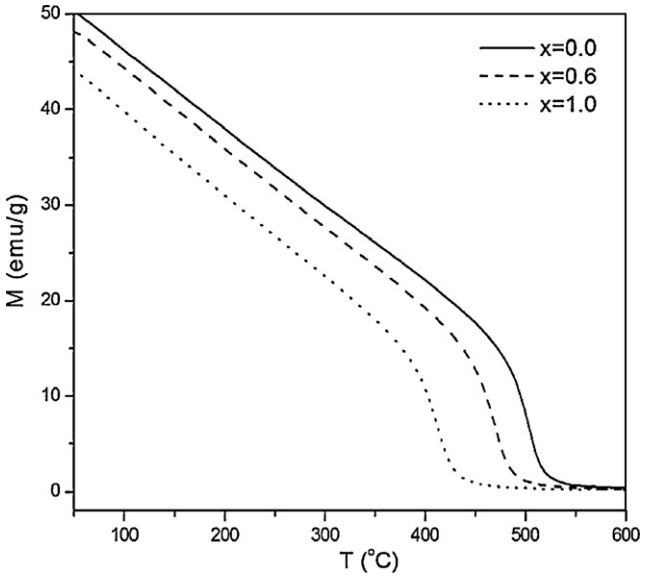

Fig. 7. Magnetization versus temperature for representative samples of $BaFe_{12-x}Ga_xO_{19}$.

demonstrated by the sharp peaks very close to T_c. These peaks are indicative of the presence of superparamagnetic particles in these samples [31]. The shift of the peak position to lower temperature with Ga substitution is consistent with the reduction in T_c. The sharpness of the peaks indicates a narrow particle size distribution, and the fact that the peaks of the two samples are of similar widths indicate that the particle size distribution is similar for the pure and doped samples. We further calculate the particle diameter following the theoretical calculations in [31] (Eq. (2)), and assuming spherical particles. For the sample with $x = 0$, the blocking temperature of the smallest particles is 470 °C (the point at which the magnetization starts rising due to unblocking these particles) and the anisotropy field at this temperature is 6285 Oe (adopting the data in Fig. 1 of [31] for the temperature variation of the anisotropy field). These values give a lower limit of the particle diameter of 29 nm. For the sample with $x = 1.0$, the blocking temperature of the smallest particles is 370 °C and the anisotropy field at this temperature is 7000 Oe, which indicate that the lower limit of particle diameter is 27 nm. These results are consistent with the TEM images of the two samples. On the other hand, the magnetization curve for the pure sample annealed at 1350 °C does not show Hopkinson peak, indicating that this higher annealing temperature leads to appreciable growth of the particles such that all particles in this sample are blocked below T_c.

4. Conclusions

Barium hexaferrite nanoparticle systems doped with different concentrations of Ga are prepared by ball milling and annealing at 1100 °C. XRD patterns for all samples show single hexagonal phase with crystallite size ranging between 37 nm and 45 nm. TEM images for the two extreme samples (with $x = 0$ and $x = 1.0$) show average particle diameters of 42 ± 13 nm and 41 ± 13 nm, respectively. The calculated lower limits of the particle diameters for these two samples are 29 nm and 27 nm, respectively. All these values are consistent and suggest that the samples consist of single-crystal, single magnetic domain particles. The pure sample annealed at 1350 °C show bulk magnetic properties, indicating that this annealing temperature is not appropriate for the synthesis of nanoparticles. The saturation magnetization for the samples

annealed at 1100 °C decreases slowly with x up to 0.6, and then drops at a faster rate for higher x values, a result suggesting that the preferential site occupation of Ga below this particular concentration is different than at higher concentration. The effect of Ga substitution for Fe results in an increase in the coercivity for $x \geq 0.2$, which is attributed to the attenuation of the magnetic exchange coupling. The reduction in exchange coupling is confirmed by the broadening of SFD and the decrease in remanence ratio and Curie temperature with increasing Ga concentration.

References

[1] J. Qiu, L. Lan, H. Zhang, M. Gu, J. Alloys Compd. 453 (2008) 261.
[2] M. Han, Y. Ou, W. Chen, L. Deng, J. Alloys Compd. 474 (2009) 185.
[3] A. Mali, A. Ataie, J. Alloys Compd. 399 (2005) 245.
[4] S. Chaudhury, S.K. Rakshit, S.C. Parida, Z. Singh, K.D. Singh Mudher, V. Venugopal, J. Alloys Compd. 455 (2008) 25.
[5] U. Topal, H. Ozkan, L. Dorosinskii, J. Alloys Compd. 428 (2007) 17.
[6] U. Topal, H. Ozkan, K.G. Topal, J. Alloys Compd. 422 (2006) 276.
[7] A. Ataie, S.E. Zojaji, J. Alloys Compd. 431 (2007) 331.
[8] K.S. Moghaddam, A. Ataie, J. Alloys Compd. 426 (2006) 415.
[9] T. Yamauchi, Y. Tsukahara, T. Sakata, H. Mori, T. Chikata, S. Katoh, Y. Wada, J. Magn. Magn. Mater. 321 (2009) 8.
[10] A. Ghasemi, A. Morisako, J. Alloys Compd. 456 (2008) 485.
[11] X. Tang, Y. Yang, K. Hu, J. Alloys Compd. 477 (2009) 322.
[12] G. Litsardakis, I. Manolakis, K. Efthimiadis, J. Alloys Compd. 427 (2007) 194.
[13] D. Ravinder, P. Shalini, P. Mahesh, K.K. Rao, M. Vithal, B.S. Boyanov, J. Alloys Compd. 364 (2004) 17.
[14] G.B. Teh, N. Saravanan, D.A. Jefferson, Mater. Chem. Phys. 105 (2007) 253.
[15] F. Tabatabaie, M.H. Fathi, A. Saatchi, A. Ghasemi, J. Alloys Compd. 474 (2009) 206.
[16] Ch. Venkateshwarlu, Ch. Ashok, B.A. Rao, D. Ravinder, B.S. Boyanov, J. Alloys Compd. 426 (2006) 1.
[17] M.J. Iqbal, M.N. Ashiq, P.H. Gomez, J. Alloys Compd. 478 (2009) 736.
[18] F. Tabatabaie, M.H. Fathi, A. Saatchi, A. Ghasemi, J. Alloys Compd. 470 (2009) 332.
[19] International Centre for Diffraction Data (ICDD), JCPDS File 43-0002.
[20] B.E. Warren, X-Ray Diffraction, Addison-Wesley, Reading, MA, 1969.
[21] H.P. Klug, L.E. Alexander, X-Ray Diffraction Procedures for Polycrystalline and Amorphous Materials, Wiley, New York, 1967.
[22] L. Rezlescu, E. Reslescu, P.D. Popa, J. Magn. Magn. Mater. 193 (1999) 288.
[23] S.Y. An, I.B. Shim, C.S. Kim, J. Appl. Phys. 91 (10) (2002) 8465.
[24] P. Sharma, R.A. Rocha, S.N. de Medeiros, A. Paesano Jr., J. Alloys Compd. 443 (2007) 37.
[25] S. Ounnunkad, P. Winotai, J. Magn. Magn. Mater. 301 (2006) 292.
[26] S.Y. An, I.B. Shim, C.S. Kim, J. Appl. Phys. 91 (10.) (2002).
[27] X.Z. Zhou, A.H. Morrish, Z.W. Li, Y.K. Hong, IEEE Trans. Magn. 27 (1991) 4654.
[28] J.M. Williams, J. Adetunji, M. Gregori, J. Magn. Magn. Mater. 220 (2000) 124.
[29] X. Zhang, Y. Duan, H. Guan, S. Liu, B. Wen, J. Magn. Magn. Mater. 311 (2007) 507.
[30] B.A. Jones, M. El-Hilo, K. O'Grady, J. Magn. Magn. Mater. 272–276 (2004) e517.
[31] H. Pfeiffer, W. Schüppel, J. Magn. Magn. Mater. 130 (1994) 92.